Talanta 117 (2013) 176–183

Contents lists available at ScienceDirect

Talanta

journal homepage: www.elsevier.com/locate/talanta

Biological application of laser induced breakdown spectroscopy technique for determination of trace elements in hair

Elshaimaa M. Emara [a], Hisham Imam [a,*], Mouyed A. Hassan [b], Salah H. Elnaby [a]

[a] National Institute of Laser Enhanced Sciences, Cairo University, Giza, Egypt
[b] College of Engineering, Gulf University, Kingdom of Bahrain, Bahrain

ARTICLE INFO

Article history:
Received 18 June 2013
Received in revised form
25 August 2013
Accepted 27 August 2013
Available online 7 September 2013

Keywords:
Hair
LIBS
Trace elements

ABSTRACT

Analysis of trace elements in mammalian hair has the potential to reveal retrospective information about an individual's nutritional status and exposure. As trace elements are incorporated into the hair during the growth process, longitudinal segments of the hair may reflect the body burden during growth. Using LIBS technique, Na, K, Ca, Mg, Si, Fe, Pb and Zn were detected in a single strand of horse hair. The results obtained through LIBS technique on hair samples were compared with the traditional technique (AAS) on digested acidified solution of the same samples. The effects of the experimental parameters on the emission lines were studied and the local thermodynamic equilibrium (LTE) in produced plasma was investigated. The transient plasma condition was verified at specific time region (1500–2000 ns) in the plasma evolution corresponding to its dynamic expanding characteristic. The relative mass concentrations of Fe and Zn were calculated by setting the concentration of C as the calibration. The information obtained from the trace elements' spectra of horse hair in this study substantiates the potential of hair as a biomarker.

1. Introduction

Every part of the mammalian body contains at least few atoms of every stable element in the periodic table. A large number of these elements are found in detectable amounts in biological samples such as blood, urine and hair. In particular, hair contains higher concentration of many of these elements. Trace elements accumulate in hair at concentrations that are generally higher than those present in other biological samples which provide a continuous record of nutrient mineral status and exposure to heavy metal pollutants as well as a probe of physiological functions. Hair has several characteristics of an ideal tissue in that it is painlessly removed, normally discarded, easily collected and its contents can be analyzed relatively easily [1].

Hair tissue mineral analysis (HTMA) is one of the most widespread techniques for the screening of metal poisoning in individuals exposed to occupational or environmental risks. In addition to its potential as a biomarker, the analysis of hair samples has several advantages. Hair is easily collected and does not require any special storage or preservation. Most recently, this analysis has been extended to the analysis of non-poisonous elements in hair since it is believed that the amount of mineral content of the hair can give an insight of the general health condition of the subject. The primary component of hair is the protein keratin, which makes it stable and robust. Also, many trace elements accumulate in hair at concentrations at least ten times higher than in blood serum or urine [2].

The equipments used for the analysis typically involve sophisticated and costly analytical instruments such as the Inductively Coupled Plasma Mass Spectrometer (ICP-MS) and Atomic Absorption Spectroscopy (AAS). These kinds of instruments guarantee very high sensitivity, with limits of detection as low as few parts per million. However, it was reported in the related literature that the absence of defined standards for instrument calibration associated with the great natural variability of hair composition may often lead to inaccuracies and huge discrepancies between different laboratories [3].

Laser Spark Spectroscopy (LASS), Laser-Induced Plasma Spectroscopy (LIPS) or as it is more often known as Laser-Induced Breakdown Spectroscopy (LIBS) is a form of atomic emission spectroscopy in which a pulsed laser is used as the excitation source. It is considered as a new trend for remote and non-invasive analysis as well as characterization and identification of hazardous materials. Few years ago several authors proposed the use of laser-induced breakdown spectroscopy (LIBS) technique for hair analysis [4]. In principle, the use of laser techniques for HTMA offers some well-defined advantages with respect to traditional ICP-MS systems in terms of the cost of analysis and operation, also the lack of necessary pretreatment of the samples and the possibility of studying the variation in concentration of the mineral elements in different points of the same single hair strand.

* Corresponding author. Tel.: +202- 111 337 0398; fax: +202- 35 731667.
E-mail address: Hishamimam@niles.edu.eg (H. Imam).

0039-9140/$ - see front matter © 2013 Elsevier B.V. All rights reserved.
http://dx.doi.org/10.1016/j.talanta.2013.08.043

The aim of the present work is to investigate the possibility of using LIBS as a new, non-invasive and promising tool for detection of trace elements in biological tissues such as hair samples which represent a chemically inert and highly mineralized tissue that has been approved recently by the US Environmental Protection Agency and the International Atomic Energy Agency for measuring the levels of toxic and essential metals in mammals. The main target of this paper is to optimize the key measurement parameters as well as determining its physical parameters such as electron density and plasma temperature to verify the LTE condition at the plasma produced by laser.

2. Materials and methods

2.1. Hair sampling

Hair samples 5–10 cm long were cut with stainless steel scissors without vanadium from horse tail and stored in plastic bags.

Once in the laboratory hair samples were washed according to the IAEA Advisory Group (International Atomic Energy Agency) following the sequence acetone-three times water–acetone to remove surface dirt and grease [5–8]. After washing, each hair sample was divided into two groups one for measurement by LIBS technique and the other for measurement by AAS technique.

Samples for the AAS measurement were cut into smaller pieces with a sterile surgical scalpel to enhance the washing procedure. The washed samples were individually placed in 30 ml crucible, dried for 24 h at 60 °C in a drying oven and then weighed. Hair samples were transformed to ash by burning in a muffle furnace for 16 h at 550 °C according to the method described by Subramanian [8]. Three ml of HNO_3 were added to each hair sample and digested. After digestion the solutions were properly diluted by the addition of Milli-Q demineralized water to reach a volume of 25 ml. Measurements were done using flame atomic absorption spectrophotometer (Thermo Scientific ICE 3500, UK) equipped with double beam and deuterium background correction. Analytical blanks were run in the same way as the samples and concentrations were determined using standard solutions prepared in the same acid matrix. All reagents used were of analytical grade (Merck). The goal was to elaborate easier analytical procedure without additional steps of extraction of exogenous contaminants from hair.

2.2. Experimental setup

The experimental setup used for the LIBS measurements of hair samples is sketched in Fig. 1.

To perform the hair analysis, the beam of a Nd:YAG pulsed laser operating at 1064 nm and delivering 100 mJ on the sample surface in about 8 ns FWHM at a maximum repetition rate of 10 Hz and a laser pulse duration of 10 ns is focused with a short focal-length 50 mm lens on a single hair strand held in front of the laser by U-shaped holder. The focal spot of the laser on the hair is approximately 50 μm in diameter with irradiance at the focal spot of approximately 10^{11} W/cm^2. The hair sample was mounted on a three-axis motorized stage controlled manually for adjustment of focusing position and scanning along the hair length.

The spectral signal resulting from the instant ablation and ionization of the hair sample is collected with UV-graded optical system (numerical aperture 0.125) at 45° with respect to the direction of the laser beam and sent through an optical fiber to the entrance of Echelle spectrometer coupled with an intensified CCD camera that provides the entire time-resolved near-ultraviolet-near-infrared spectrum in a single laser shot with a constant relative spectral resolution of $\lambda/\Delta\lambda = 3100$.

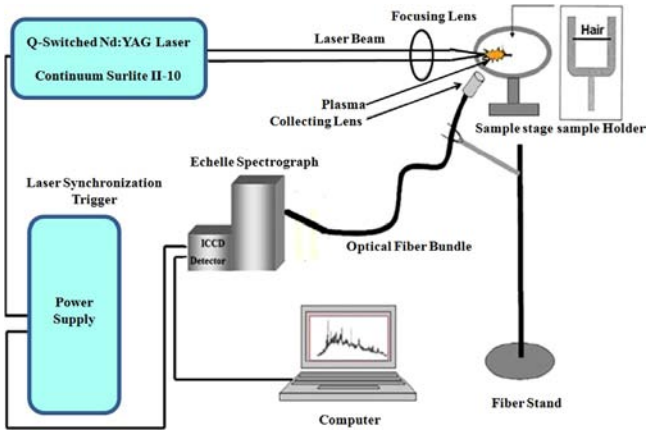

Fig. 1. The Experimental LIBS setup.

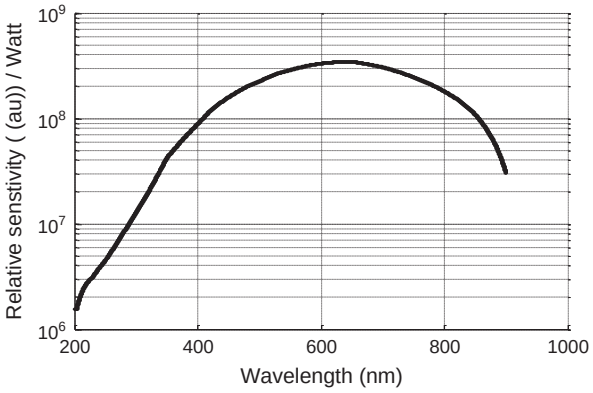

Fig. 2. Variation of the spectral sensitivity of the experimental setup to the intensity over the entire wavelength region of the setup.

The wavelength scale was calibrated using a low pressure Hg-lamp (Ocean optics). The instrumental bandwidth was measured from the FWHM of the Hg lines and was found on the average of 0.12 ± 0.02 nm. Identification of the different lines in the LIBS spectrum was carried out using Gram32 software program. A low pressure Deuterium–Halogen lamp type (Ocean optics, model DH-2000-CAL) was used in calibrating the emission spectral intensities (relative sensitivity) against the Echelle spectrograph and camera gate time window was extrapolated to the actually set (2 μs) value during the experimental investigation of LIBS as indicated in Fig. 2.

The detection process was computer controlled using licensed software (Winspec32) to perform linear scanning of the hair length, spectral averages and the acquisition of the spectra. In typical experimental conditions the LIBS spectra are taken in a single laser shot from 500 ns to 10000 ns after the laser pulse with a measuring gate width of 5000 ns and the complete determination of hair composition was performed in less than 2 min. These choices perform a good LIBS signal in a regime where the continuum emission of the plasma is substantially decayed where space and time variations of plasma parameters are almost negligible. A series of 50 LIBS spectra were typically taken along the hair length (few millimeters were sufficient since the hair in general did not break as a consequence of the laser irradiation). The LIBS spectra manipulations were performed using OriginPro8 software program [9] which allows the qualitative and quantitative determination of the elemental composition of the hair as indicated in Fig. 3.

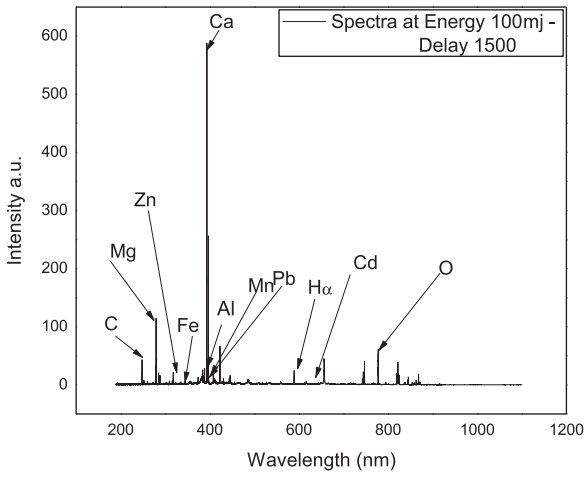

Fig. 3. Spectra of the detected elemental horse hair contents at E of 100 mj and delay of 1500.

3. Results and discussion

The results obtained using single pulse LIBS technique for detection of trace elements in horse hair samples were comparable with respect to the AAS technique.

In the present work qualitative and quantitative analysis were established for the obtained experimental data of the single pulse LIBS with different gate time delays. The effect of different delays on the same sample was obtained at different shots as well as the plasma parameters such as plasma temperature and electron density. The limit of detections for Ca and Fe were calculated at the optimum experimental parameters.

3.1. Qualitative analysis

Qualitative analysis was used to detect the presence of trace elements in hair samples where the plasma spectrum showed information about these elements in the sample. This information was in the form of emission lines located at specific wavelengths as well as the intensity and the relative intensities of the lines which are important for analyzing the samples and for detection of heavy metals.

3.1.1. Emission spectra

The emission spectra of LIBS experiments have been collected at different pulse shots (number of shots were 20 and 50).

The obtained LIBS spectra lines at different gate delays (500–10000 ns) and fixed gate width of 5000 ns showed sharp lines with high intensity values as indicated in Fig. 4. There were some variations of spectral line intensity values due to the long life-time of the plasma in atmospheric air pressure as the duration of the plasma shots ranged between 20 and 100 μs according to the used laser energy. The background continuum emission is clear at the early stages of plasma evolution (at short delay times), due to the combination of Bremsstrahlung radiation and emission from incandescent particles ablated from the target sample.

Different gate delays were used with accumulation number of 20 and 50 shots as indicated in Fig. 4a–d. The gate width was studied at 1 μs and 5 μs. The sample was moved every 5 laser shots to ensure generating plasma on a fresh surface and to detect emission lines along the hair strand. The gate time delay showed strong effect on the spectral lines (atomic and ionic) where the trace elements intensities were obvious between 500 ns and 2000 ns delays but these intensities decayed rapidly between 3000 ns and 10000 ns.

The effective lifetimes of the emission lines of C I, Ca I, II and Fe I, II were investigated by the time-resolved LIBS technique to determine the suitable experimental parameters. Figs. 5–7 show the effect of the gate time delays on the temporal evolution of integrated intensity for spectral lines of Fe I 344.06, Fe II 273.94, Ca I 430 and Ca II 393.

At 20 shots, the atomic spectral line intensities of Fe and Ca were decayed after gate time delay of 1030.47 ns and 949.072 ns respectively. At 50 shots, these intensities were decayed after gate time delay of 1174.15 ns and 1013.122 ns. It was obvious that the spectral lines decayed almost similarly at 20 and 50 shots.

For the ionic spectral lines of Fe and Ca the intensities decayed after 801.12 ns and 1484.08 ns gate time delay at 20 shots meanwhile they decayed after 1096.53 ns and 1387.48 ns at 50 shots respectively.

So it was obvious that the ionic spectral lines decayed more rapidly than the atomic ones in case of iron (Fe) which could be explained by the additional amount of atoms produced due to the electron recombination with ions during plasma cooling time [10]. The ionic lines decrease exponentially with increasing the gate delay in a more uniform behavior with respect to the atomic ones. According to Figs. 5 and 6, the ionic lines seem to have much higher peak values compared to the atomic ones which give an indication of suffering a strong self-absorption.

Therefore the lifetimes of the spectral lines emission can be derived directly from the solid curves. As shown in Figs. 5–7 the fitted lifetime values are $\approx$1500 ns, $\approx$1000 ns and $\approx$1300 ns for C, Ca and Fe excited atoms, respectively. It was obviously that the lifetimes of excited atoms are quite short and intensities of the spectral lines are rather weak when the delay is 1.5 μs. It means that the acquisition should start in 1.5–2 μs from the impacting of laser pulse for strong intensities of the emission lines of C, Ca and Fe atoms. However the influence of the broad background continuum from the luminous plasma should be considered carefully during this time.

The optimal observed time delay depends on the laser pulse energy, the kind of sample as well as the surrounding atmosphere [11]. The present work indicates that the optimum conditions for such experiment are gate time delays between 1000 and 2000 ns with gate width of 5000 ns at fixed pulse energy of 100 mJ.

3.2. Evaluation of the plasma parameters

The analytical measurements in the present study were carried out under local thermo-dynamic equilibrium (LTE) conditions. To verify the LTE, the electron density (N_e) and electron temperature (T_e) must be estimated as well as the study of the temporal behavior of them with dynamic processes.

3.2.1. Plasma electron density

One of the most powerful spectroscopic techniques to determine the electron density with reasonable accuracy is the measurement of the Stark broadening profile of the atomic emission lines. In the present work, the hydrogen lines H_α at 656.27 nm was chosen for the electron density measurements. At the beginning of measurements it was much better to fit the obtained experimental profiles of H_α line by a best fitting procedure then performing an appropriate de-convolution of Voigt profile as shown in Fig. 8.

In accordance with the standard theory of Stark broadening of the hydrogenic lines [12,13] neglecting contributions due to atomic and ionic impacts, the line width ($\Delta\lambda_{1/2}$) of the H_α-line is correlated with the plasma electron density n_e as:

$$n_e(H_\alpha) = 8.02 \times 10^{12} \left(\frac{\Delta\lambda_{1/2}}{\alpha_{1/2}}\right)^{3/2} \text{cm}^{-3} \quad (1)$$

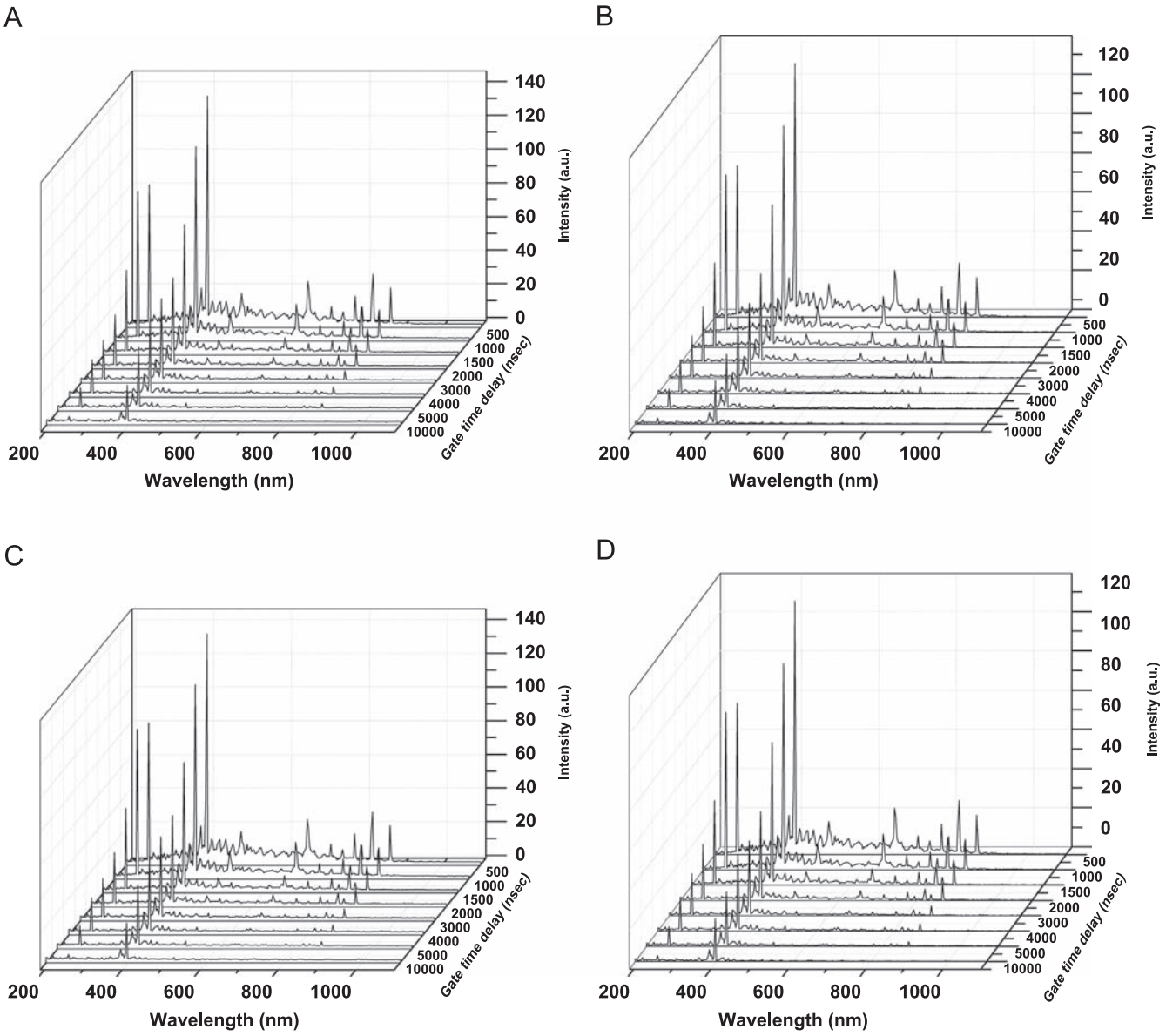

Fig. 4. a: LIBS spectra from single pulse with gate delays (500–10000 ns) at fixed gate width of 1000 ns at 20 shots. b: LIBS spectra from single pulse with gate delays (500–10000 ns) at fixed gate width of 1000 ns at 50 shots. c: LIBS spectra from single pulse with gate delays (500–10000 ns) at fixed gate width of 5000 ns at 20 shots. d: LIBS spectra from single pulse with gate delays (500–10000 ns) at fixed gate width of 5000 ns at 50 shots.

where $\Delta\lambda_{1/2}$ is the FWHM of the line in Å and $\alpha_{1/2}$ is the half width of the reduced Stark profiles in Å. It is a weak function of electron density and temperature through the ion-ion correlation, Debye-shielding correction and the velocity dependence of the impact broadening. Precise values of ($\alpha_{1/2}$) for the Balmer series are indicated in [12,13]. The obtained electron density values of H_α lines were plotted as a function of different gate delays (0.5–10 μs) at fixed gate delay width (5 μs) and number of laser shots (20 and 50) as shown in Fig. 9.

It was found that the electron density exponentially decay with time that can be attributed to electron-ion recombination as the plasma cool down with time and because no more energy is pumped into plasma after the termination of the laser pulse. Little or no change in electron density has been found due to the change in number of shots as shown in Fig. 9.

3.2.2. Plasma temperature

The measurement of the electron temperature can be done through either of the following methods namely; the relative intensity of two or more lines emerging from the same kind of species and the same ionization stage or more general the Boltzmann plot [14–16]. Certain critical conditions should be fulfilled such as (i) the wavelength separation must be very small in order to avoid the corrections against the relative response of the detector (ii) the upper excited state energy separation should be as large as possible to get high precision and (iii) the lines should be optically thin. Of course the lines intensities should be corrected against the relative response factors of the detector. The spectral lines which were analyzed in this work are listed in Table 1. The table summarizes the wavelength of the lines selected for this study, their corresponding electronic configuration, the energy E, statistical weights g of the upper (k) level and the transition probability A_{ki}. For the evaluation of the plasma temperature via the Boltzmann plot method it is important to verify that the plasma is not optically thick for the detectable lines.

The self-absorption coefficient at the line center (λ_o) can be defined as the ratio of the intensity (counts per s) of a spectral line subjected to self-absorption to that of the same line in the limit of

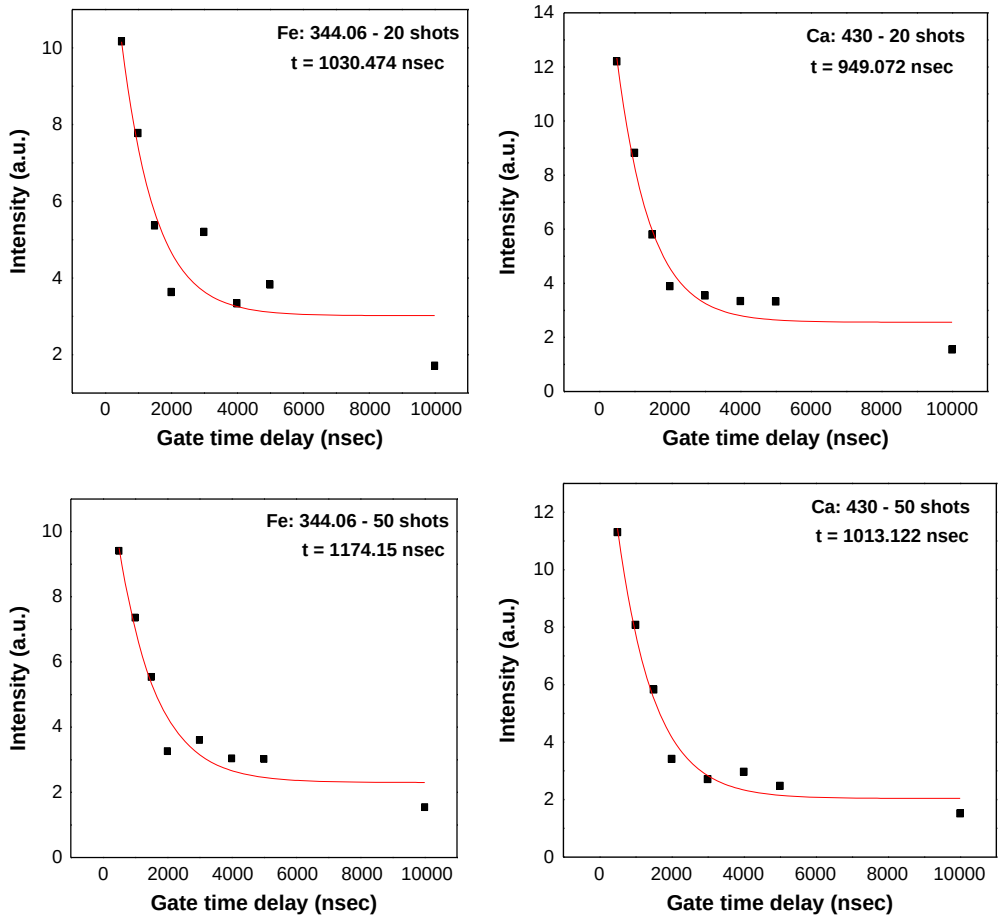

Fig. 5. The effect of different gate time delays on atomic spectral lines of Fe and Ca.

negligible self-absorption and can be calculated from [17]:

$$SA = \frac{I(\lambda_0)}{I_o(\lambda_o)} = \frac{1-e^{-k(\lambda_o)l}}{k\,(\lambda_o)\,l} = \left(\frac{\Delta\lambda_1}{\Delta\lambda_0}\right)^{1/\alpha} = \left(\frac{n_e^1}{n_e^{H_\alpha}}\right) \quad (2)$$

where I_o (λ_o) is the intensity of the line (counts per s) at the central wavelength (λ_o) in the limit of negligible self-absorption (which often occurs in the very small concentrations of the analyzed emitting atoms) and I (λ_o) is the experimentally measured line height (counts per s) of the same line in the presence of self-absorption [17]. Eq. (2) indicates that the SA coefficient varies from 1 in case of optically thin line to the limit of zero in case of completely self absorbed line [17]. This effect of self-absorption was treated using Eq. (2) and the line intensity was corrected also using the same equation, so as to give the values of the intensity with the assumption of no self-absorption. These procedures were done with the result of the Boltzmann plot for atomic lines of iron.

Plasma temperature values were plotted as a function of gate delays. It can be observed that the plasma temperature decreases exponentially by increasing the gate delay with slow variation (e.g. from 8000 to 6000 K at 500–10000 ns, respectively) as shown in Fig. 10.

The simple criterion of McWhirter formula [15] has been applied for judging the existence of LTE in the present work. Substituting McWhirter formula with the temperature values previously calculated from Boltzmann equations, a value for the electron density (N_e) less than electron density calculated from Stark method was obtained. This means that the LTE conditions are valid over a range of delays. As pointed out in the publication [18] the McWhirter formula is necessary but not sufficient for the validity of the LTE assumption in case of laser-induced plasma. Therefore two additional criteria should be verified for LTE validity especially for transient and inhomogeneous plasma as mentioned by Griem [16]. In the present work the obtained plasma assumed to be homogeneous according to the confinement effect. Therefore only the transient plasma condition needs to be verified. However the present plasma parameters varied with small change over the selected experimental parameter (i.e. gate delay and McWhirter criterion is fulfilled) which means the plasma evolves through quasi equilibrium near LTE states. Nevertheless for successfully checked LTE plasma transient plasma criterion is needed to the validity of LTE. The relaxation time of plasma (time needed for the establishment of excitation and ionization equilibrium) is shorter than the variation time of plasma parameters. The relaxation processes of these spectral lines' emission were obtained and demonstrated in Figs. 5–7. The lifetimes of excited atoms ranged between 1500 and 2000 ns. The temporal evolution of N_e and T_e diminished exponentially with time at 2000–2500 ns, respectively as shown in Figs. 9 and 10. This can be true locally and for specific time region (1500–2000 ns) in the plasma evolution corresponding to its dynamic expanding characteristics [19].

3.3. Quantitative analysis

The present work used both AAS and LIBS techniques as two different spectroscopic techniques to identify and quantify some trace elements in horse hair. The quantity of trace elements C, Zn and Fe in the horse samples were analyzed using AAS technique. Carbon is the dominant element in mammalian hair. The relative mass concentrations of Fe and Zn were calculated by

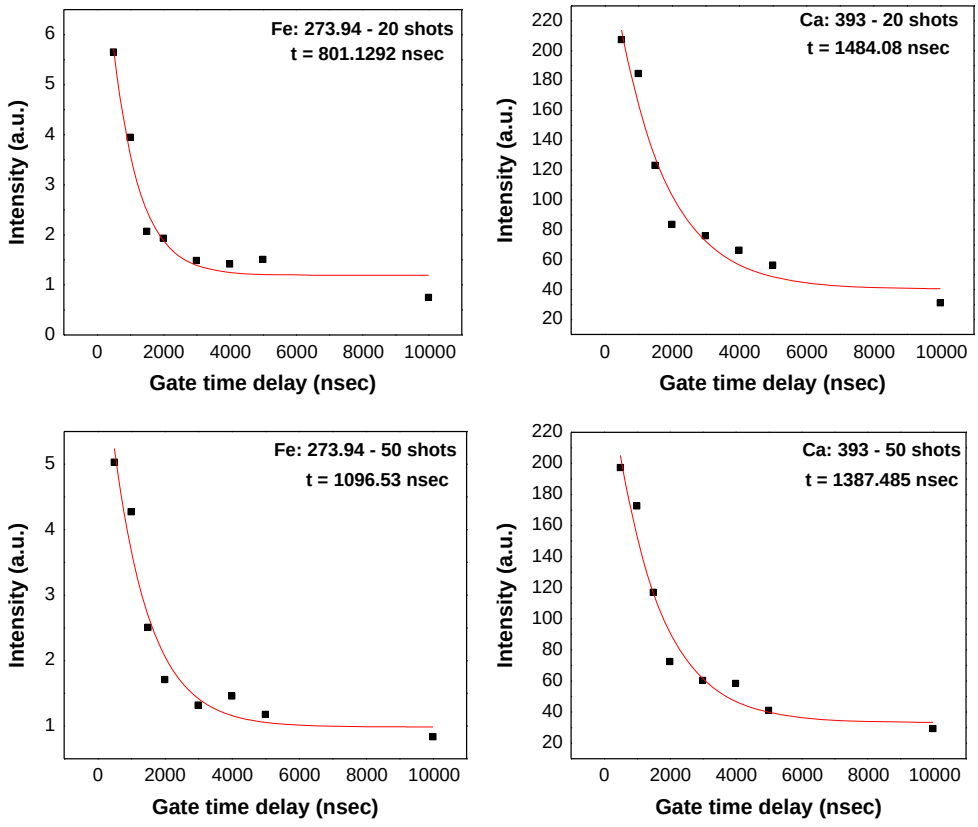

Fig. 6. The effect of different gate time delays on ionic spectral lines of Fe and Ca.

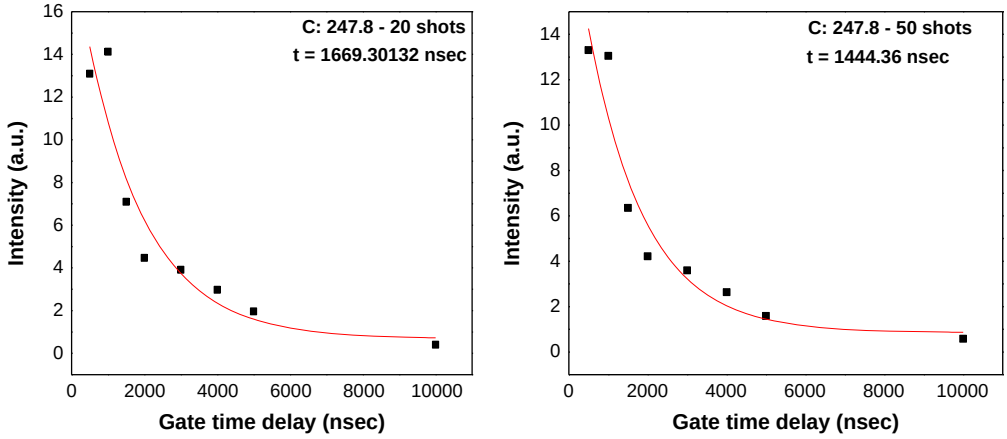

Fig. 7. The effect of different gate time delays on atomic spectral lines of C.

setting the concentration of C as the reference element. The relative mass concentrations using AAS technique were 2.1% for Fe and 0.23% for Zn.

On the other hand laser-produced plasmas obtained on the horse hair for the quantitative analysis of trace elements showed more feasibility. The wavelengths of interest were 247.8 nm for C, 344.78 nm for Fe and 334.5 nm for Zn because only atomic and single ionization lines were observed. The relative mass concentration for selected elements was calculated as the ratio number of atoms and ions for the selected elements to reference element. The elemental number densities were estimated using Boltzmann and Saha Equations [15] with the aid of the values of plasma temperature and electron density. The relative mass concentrations using LIBS technique were 1.78% for Fe and 0.26% for Zn. The data obtained using both techniques showed non-significant difference (statistical t-test at $p < 0.01$).

4. Conclusion

The elements Na, K, Ca, Mg, Si, Fe, Pb and Zn in a single strand of horse hair were determined by LIBS technique. The analytical measurements in the present study were carried out under local thermo-dynamic equilibrium (LTE) conditions. To verify the LTE we estimated the electron density (N_e) and electron temperature (T_e) and studied the temporal behavior of them with dynamic

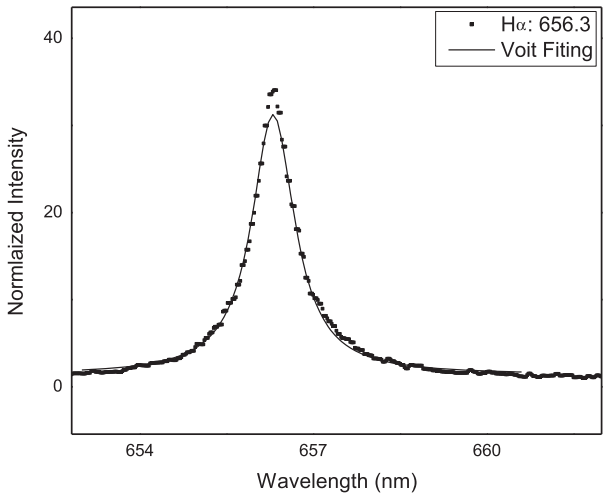

Fig. 8. Normalized theoretical Voigt profile for H_α line.

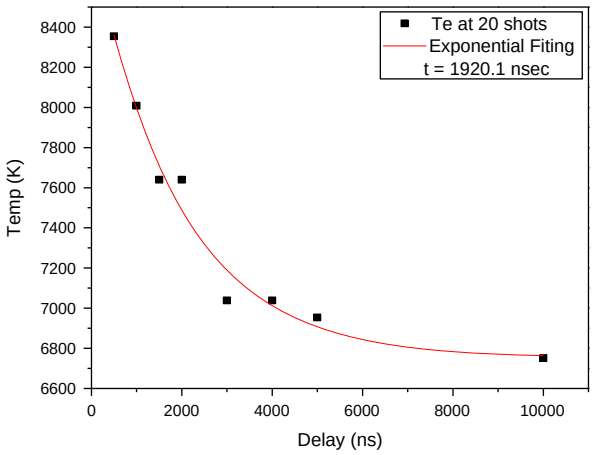

Fig. 10. Temporal behavior of the plasma temperature obtained via Boltzmann equation.

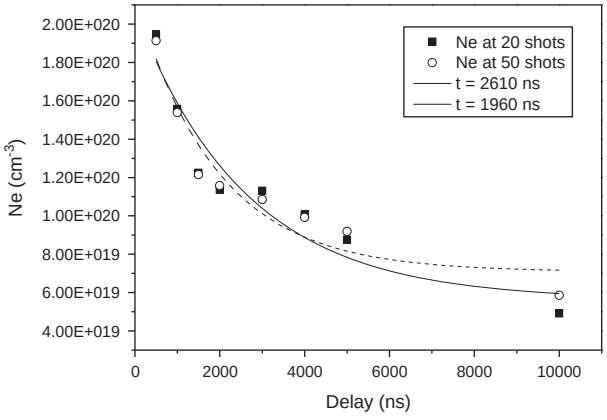

Fig. 9. Temporal evaluation of Ne at 20 and 50 laser shots.

Table 1
The spectroscopic constants for Fe, Ca, Zn and C.

Species	λ (nm)	Transition	A_k (s^{-1}) × 10^8	E_k (eV)	g_k
Fe I	370.55	$3p^63d^64s^2$–$3p^63d^6(^5D)4s4p(^3P^\circ)$	0.0322	3.396	7
	371.99	$3p^63d^64s^2$–$3p^63d^6(^5D)4s4p(^3P^\circ)$	0.162	3.332	11
	372.25	$3p^63d^64s^2$–$3p^63d^6(^5D)4s4p(^3P^\circ)$	0.0497	3.416	5
	373.48	$3p^63d^7(^4F)4s$–$3p^63d^7(^4F)4p$	0.902	4.177	11
	374.56	$3p^63d^64s^2$–$3p^63d^6(^5D)4s4p(^3P^\circ)$	0.115	3.396	7
	375.82	$3p^63d^7(^4F)4s$–$3p^63d^7(^4F)4p$	0.634	4.256	7
	376.38	$3p^63d^7(^4F)4s$–$3p^63d^7(^4F)4p$	0.544	4.283	5
	376.55	$3p^63d^7(^2H)4s$–$3p^63d^7(^2H)4p$	0.98	6.528	15
	376.71	$p^63d^7(^4F)4s$–$3p^63d^7(^4F)4p$	0.64	4.301	3
Ca I	422.673	$3p^64s^21S$ - $3p^64s4p(1P^\circ)$	2.18	2.932	3
	429.899	$3p^64s4p(^3P^\circ)$–$3p^64p^2(3P)$	0.466	4.77	3
	430.253	$3p^64s4p(^3P^\circ)$–$3p^64p^23P$	1.36	4.787	5
	430.774	$3p^64s4p(^3P^\circ)$–$3p^64p^23P$	1.99	4.763	1
Ca II	393.366	$3p^64s\ 2S$–$3p^64p\ (^2P^\circ)$	1.47	3.151	4
	396.847	$3p^64s\ ^2S$–$3p^64p\ (^2P^\circ)$	1.4	3.123	2
Zn I	328.2	$4s4d\ ^3D1$–$4s4p\ (^3P^\circ)$	0.866	7.7823	3
	330.3	$4s4d\ ^3D2$–$4s4p\ (^3P_1)$	1.07	7.783	5
	334.5	$4s4d\ ^3D3$–$4s4p\ (^3P_2)$	1.5	7.783	7
C I	247.856	$2s^22p^2\ ^1S$–$2s^22p3s(^1P^\circ)$	0.280	7.685	3

processes. The relaxation processes of spectral lines' emission and the lifetimes of excited atoms were obtained. We found that the relaxation time of plasma was shorter than the variation time of plasma parameters. This can be true locally and for specific time region (1500–2000 ns) in the plasma evolution corresponding to its dynamic expanding characteristics. The present plasma parameters varied with small change over the selected experimental parameters (i.e. gate delay and McWhirter criterion is fulfilled) which means the plasma evolves through quasi equilibrium near LTE states. The elemental analysis of horse hair using both LIBS and AAS techniques were statistically consistent and the LIBS data were in reasonable agreement with the AAS data.

Acknowledgment

The authors would like to thank Dr. Wael A. Omar, Associate Professor of Animal Ecology – Faculty of Science – Cairo University, for his valuable assistance in AAS sample processing and measurements.

References

[1] M. Marlowe, C. Moon, J. Errera, J. Stellern, J. Orthomol. Med. 12 (1) (1983) 26–33.
[2] T.H. Maugh, Science 202 (1978) 1271–1273, http://dx.doi.org/10.1126/science.725602.
[3] M. Corsi, G. Cristoforetti, M. Hidalgo, S. Legnaioli, V. Palleschi, A. Salvetti, E. Tognoni, C. Vallebona, Appl. Opt. 42 (30) (2003) 6133–6137, http://dx.doi.org/10.1364/AO.42.006133.
[4] V.K. Singh, A.K. Rai, Lasers Med. Sci. 26 (2011) 673–687, http://dx.doi.org/10.1007/s10103-011-0921-2.
[5] B. Nowak, Sci. Total Environ. 209 (1) (1998) 59–68, http://dx.doi.org/10.1016/S0048-9697(97)00298-2.
[6] Y.S. Ryabukin, Activation analysis of hair as an indicator of contamination of man by environmental trace element pollutants, IAEA Report, IAEA/RL/50. IAEA, Vienna, 1978.
[7] H. Sela, Z. Karpas, M. Zoriy, C. Pickhardt, J.S. Becker, Int. J. Mass Spectrom. 261 (2007) 199–207, http://dx.doi.org/10.1016/j.ijms.2006.09.018.
[8] K.S. Subramanian, Spectrochim. Acta 51(B) (1996) 291–319, http://dx.doi.org/10.1016/0584-8547(95)01425-X.
[9] OriginPro 8 SR0, v8.0724, Origin Lab Corporation, USA.
[10] A. De Giacomo, M. Dell'Aglio, F. Colao, R. Fantoni, Spectrochim. Acta 59(B) (2004) 1431–1438, http://dx.doi.org/10.1016/j.sab.2004.07.002.
[11] D.M. Diaz Pace, C.A. D'Angelo, D. Bertuccelli, G. Bertuccelli, Spectrochim. Acta 61(B) (2006) 929–933, http://dx.doi.org/10.1016/j.sab.2006.07.003.
[12] H.R. Griem, Spectral Line Broadening by Plasmas, Academic Press, New York, USA, 1974.
[13] P. Kepple, H.R. Griem, Phys. Rev. 173 (1968) 317–325, http://dx.doi.org/10.1103/physrev.173.317.
[14] H.R. Griem, Plasma Spectroscopy, McGraw-Hill Inc., New York, USA, 1964.
[15] W. Lochte-Holtgreven, Plasma Diagnostics, North-Holland Publishing, Amsterdam (1968) 135.

[16] H.R. Griem, Principles of Plasma Spectroscopy, Cambridge University Press, Cambridge, England, 1997.
[17] A.M. El Sherbini, Th.M. El Sherbini, H. Hegazy, G. Cristoforetti, S. Legnaioli, V. Palleschi, L. Pardini, A. Salvetti, E. Tognoni, Spectrochim. Acta 60(B) (2005) 1573–1579, http://dx.doi.org/10.1016/j.sab.2005.10.011.
[18] R.W.P. McWhirter, Spectral intensities, in: R.H. Huddlestone, S.L. Leonard (Eds.), Plasma Diagnostic Techniques, Academic Press, New York, 1965, pp. 201–264.
[19] W.T. Chan, R.E. Russo, Spectrochim. Acta 46(B) (1991) 1471–1486, http://dx.doi.org/10.1016/0584-8547(91)80199-D.